Chemical Science

rsc.li/chemical-science

ROYAL SOCIETY
OF CHEMISTRY

EDGE ARTICLE
Christopher Barner-Kowollik, Peter W. Roesky *et al.*
Heterobimetallic Eu(III)/Pt(II) single-chain nanoparticles:
a path to enlighten catalytic reactions

EDGE ARTICLE

Check for updates

Heterobimetallic Eu(III)/Pt(II) single-chain nanoparticles: a path to enlighten catalytic reactions †

Nicolai D. Knöfel, [a] Hannah Rothfuss, [b] Pavleta Tzvetkova, [d] Bragavie Kulendran, [a] Christopher Barner-Kowollik *[bc] and Peter W. Roesky *[a]

We introduce the formation and characterization of heterometallic single-chain nanoparticles entailing both catalytic and luminescent properties. A terpolymer containing two divergent ligand moieties, phosphines and phosphine oxides, is synthesized and intramolecularly folded into nanoparticles *via* a selective metal complexation of Pt(II) and Eu(III). The formation of heterometallic Eu(III)/Pt(II) nanoparticles is evidenced by size exclusion chromatography, multinuclear NMR (^{1}H, ^{31}P{^{1}H}, ^{19}F, ^{195}Pt) as well as diffusion-ordered NMR and IR spectroscopy. Critically, we demonstrate the activity of the SCNPs as a homogeneous and luminescent catalytic system in the amination reaction of allyl alcohol.

Introduction

Single-chain nanoparticles (SCNPs) are single polymer chains, which – *via* defined introduction of functionalized motifs – can be intramolecularly folded into highly specific nanoparticles.[1–4] Employing metal ions as linker molecules allows for the design of task-specific pockets within the SCNP architecture in addition to the introduction of unique properties, such as catalytic activity or luminescent behavior. To date, a series of metal-folded SCNP systems has been examined in catalytic studies,[5–7] showing promising results, *e.g.* enhanced selectivity, catalyst recyclability as well as enzyme-mimetic behavior.[8–16] Synthetically challenging, yet opening advanced prospects in SCNP chemistry, the enclosure of different metal species within one chain may enable the formation of macromolecular materials with versatile functionalities. The design of compartmentalized areas within a SCNP, containing metal ions of different characteristics, may permit access to advanced catalytic reactions, such as multi-step or tandem catalysis.[13]

As a rare example, Lemcoff and colleagues designed heterobimetallic single-chain nanoparticles *via* the introduction of catalytically active Ir(I) and Rh(I) ions into a diene-functionalized polymer chain.[11] However, no targeted metal placement was carried out, as merely one type of ligand moiety was present, suitable for both metal species. Thus, the introduction of orthogonal linker moieties into the polymer chain is mandatory for a selective and controlled incorporation of different metal ions. To form heterometallic SCNP structures, at least one of the metal precursors needs to induce the chain collapse, whereas a second metal species coordinating to an orthogonal ligand system can add additional functionality. Striving for a SCNP system, which exhibits both luminescent and catalytic properties, we herein report the synthesis and in-depth characterization of a bifunctional terpolymer, featuring both phosphine and phosphine oxide ligand moieties. The terpolymer enables SCNP formation *via* orthogonal complexation of platinum(II) and europium(III), providing novel catalytic material (Fig. 1). The combinatorial design of catalytic and luminescent properties within a SCNPs system allows *i.e.* the visualization and tracking of the polymer nanoparticles during catalysis and helps to monitor a successful catalyst separation.

Results and discussion

Polymer synthesis and characterization

Ligand systems applied in metal–SCNP chemistry, mostly containing oxygen- and nitrogen-donor functionalities,[9,17–19] tend to coordinate non-selectively to metal ions. In recent studies, our teams investigated the introduction of phosphine moieties into polymer chains, which enabled subsequent SCNP formation *via* the addition of Pd(II) as well as Pt(II) ions.[8,20] Advantageously, phosphines can readily be oxidized, thereby changing their

[a]Institute of Inorganic Chemistry, Karlsruhe Institute of Technology (KIT), Engesserstrasse 15, 76131 Karlsruhe, Germany. E-mail: roesky@kit.edu

[b]Macromolecular Architectures, Institute for Chemical Technology and Polymer Chemistry, Karlsruhe Institute of Technology (KIT), Engesserstrasse 18, 76131 Karlsruhe, Germany. E-mail: christopher.barner-kowollik@kit.edu

[c]Centre for Materials Science, School of Chemistry and Physics, Queensland University of Technology (QUT), 2 George Street, Brisbane, Queensland 4000, Australia. E-mail: christopher.barnerkowollik@qut.edu.au

[d]Institute of Organic Chemistry, Institute for Biological Interfaces 4 – Magnetic Resonance, Karlsruhe Institute of Technology (KIT), Fritz-Haber-Weg 6, 76131 Karlsruhe, Germany

† Electronic supplementary information (ESI) available: NMR- and IR-spectra. See DOI: 10.1039/d0sc03579c
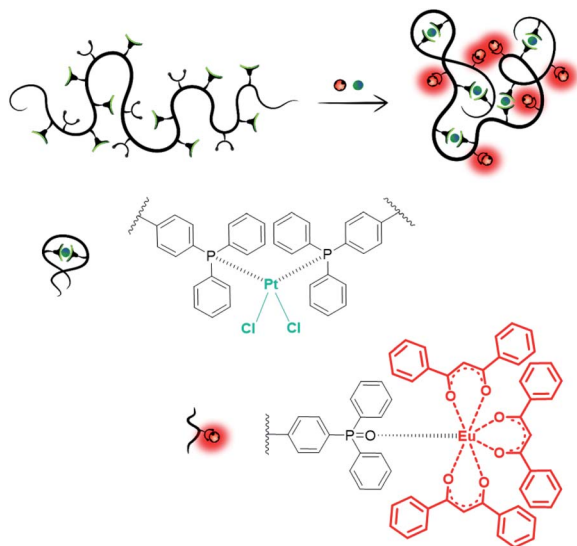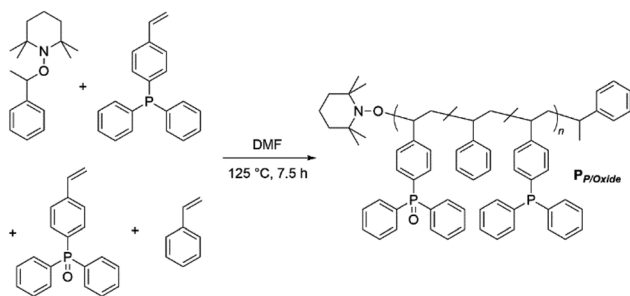
Fig. 1 Illustration of targeted heterometallic SCNPs: the incorporation of two disparate ligands in the polymer chain allows for subsequent selective metal complexation and thus generation of a 3D organized macromolecular system.

coordination behavior significantly due to the ionic character of the P=O bond.[21] In a terpolymer exhibiting both phosphine and phosphine oxide moieties, the soft phosphine ligands can selectively coordinate to Pt(II) centers, inducing the single chain collapse, whereas the phosphine oxide functionalities act as a hard acid counterpart for the complexation of luminescent Eu(III). For the synthesis of a suitable bifunctional terpolymer, the monomers 4-(diphenyl-phosphino)styrene, 4-(diphenyl-phosphino oxide)styrene and styrene, working as a spacer monomer, were copolymerized via nitroxide mediated polymerization (NMP),[22] yielding $P_{P/Oxide}$ (Scheme 1). Hereby, the phosphine and phosphine oxide functionalities are statistically distributed along the chain. The monomer composition of terpolymer $P_{P/Oxide}$ was determined by ^{1}H and $^{31}P\{^{1}H\}$ NMR spectroscopy (in CDCl$_3$), comparing the resonance integrals of the respective monomer species (ESI, Fig. S2 and S3†).

Analysis resulted in a monomer ratio of approx. 3.5 mol% phosphine and 1.7 mol% phosphine oxide functionalities in the terpolymer, in agre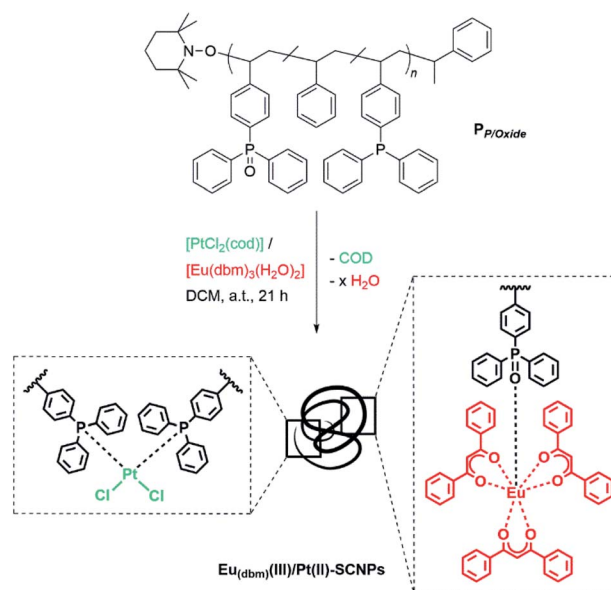ement with the feed ratio. The given values are – within the margin of error of NMR spectroscopy – estimates which are additionally hampered by the solvent resonance in the ^{1}H NMR spectrum. Therefore, $^{31}P\{^{1}H\}$ NMR experiments, applying bis(diphenyl-phosphino)methane (DPPM) as an external standard, were additionally performed and resulted in 0.17 mmol phosphine oxide and 0.35 mmol phosphine species per 1 g of terpolymer $P_{P/Oxide}$ (Fig. S21†), which is in agreement with the priorly determined values. Accordingly, two resonances, in a ratio of 2 : 1, are observed at $\delta = -6.2$ ppm and $\delta = 29.2$ ppm in the $^{31}P\{^{1}H\}$ NMR spectrum of $P_{P/Oxide}$, attributed to the implemented triarylphosphine and triarylphosphine oxide species (Fig. 4A). The characterization of $P_{P/Oxide}$ via SEC (THF, RI) resulted in M_p = 41 400 g mol^{-1} (average molecular weight 25 300 g mol^{-1}) with a dispersity of $Đ$ = 1.4 (Fig. 3, top). Combining the results of the SEC and NMR analysis, approx. 8–9 phosphine and 4 phosphine oxide moieties are estimated per chain. In addition, $P_{P/Oxide}$ was analyzed by IR spectroscopy (ESI, Fig. S22†). Among others, characteristic bands at $\tilde{\nu} = 1202$ and $\tilde{\nu} = 1118$ cm^{-1} are attributed to the P=O vibrational stretching and C–H deformation mode of the triarylphosphine oxide units.[23,24]

SCNPs formation and characterization

As phosphine ligands are capable of forming stable 2 : 1 complexes with Pt(II)-ions via coordinative bond formation, the intramolecular collapse of terpolymer $P_{P/Oxide}$ into SCNPs was induced by addition to the platinum complex [PtCl$_2$(cod)], (cod = cyclooctadiene) in high dilution (Scheme 2).

Herein, cod is readily substituted by two phosphine ligands of $P_{P/Oxide}$, as already established in previous studies on Pt(II)-linked SCNPs.[8] The orthogonal properties of the phosphine

Scheme 1 Synthesis of bifunctional terpolymer $P_{P/Oxide}$ via nitroxide mediated polymerization of styrene, 4-(diphenylphosphino)styrene and 4-(diphenylphosphino oxide)styrene.

Scheme 2 Formation of heterometallic SCNPs based on the bifunctional terpolymer $P_{P/Oxide}$ and the metal precursors [PtCl$_2$(cod)] and [Eu(dbm)$_3$(H$_2$O)$_2$] in a one-pot reaction. The metal species coordinate orthogonally to the respective ligands in the polymer scaffold, yielding fluorescent and catalytic active $Eu_{(dbm)}(III)/Pt(II)$–SCNPs.

oxide ligands, which do not coordinate to Pt(II), allow for the simultaneous complexation of a second suitable metal species. Thus, the europium precursor [Eu(dbm)$_3$(H$_2$O)$_2$] (dbm = dibenzoyl-methanide) was employed, coordinating exclusively to the phosphine oxides, *via* release of H$_2$O, yielding **Eu$_{(dbm)}$(III)/ Pt(II)–SCNPs**. Hereby, the phosphine oxide Eu(III) coordination can be realized either prior or subsequent to the Pt induced chain folding, resulting in an analogue Eu(III)–Pt(II)–SCNP system. Thus, the nanoparticle formation is independent from the sequence of metal ion addition, allowing dual functionalization and single-chain collapse in one step. Additional experiments, investigating stepwise metal addition and selective coordination behavior of platinum and europium towards the disparate ligand systems, are presented in the ESI (Schemes S4 and S5†). In theory, the attachment of either one or two phosphine oxides to a [Eu(β-diketonate)$_3$] species is possible.[25,26] However, the small number of approx. four phosphine oxide units per chain, combined with a high steric demand of the rigid polymer backbone suggests a 1 : 1 coordination ratio. In addition, the coordination of [Eu(dbm)$_3$] to a sole triarylphosphine oxide functionalized copolymer (styrene based) was investigated at high concentrations. Yet, no network formation was observed, as it is expected in case of a 2 : 1 ligand to Eu(III) coordination. For this reason, an Eu(III) coordination ratio of 1 : 1 is presumed. This assumption was further confirmed by DOSY NMR measurements (see below).

Following an analogous reaction procedure, different Eu(III) complexes can be applied, emphasizing the versatile applicability of the bifunctional polymer system. In case of the precursor [Eu(tta)$_3$(H$_2$O)] (tta = thenoyltrifluoroacetonate) heterometallic **Eu$_{(tta)}$(III)/Pt(II)–SCNPs** were obtained, exhibiting *e.g.* a convenient ^{19}F NMR sensor (Fig. 2 and ESI, Scheme S3†).

To confirm the assumption of an orthogonal metal complexation and verify the metal-induced chain compaction, the obtained particles were thoroughly investigated (for detailed analysis of the **Eu$_{(tta)}$(III)/Pt(II)–SCNPs** refer to ESI†). The expected collapse into a more compact structure was verified by
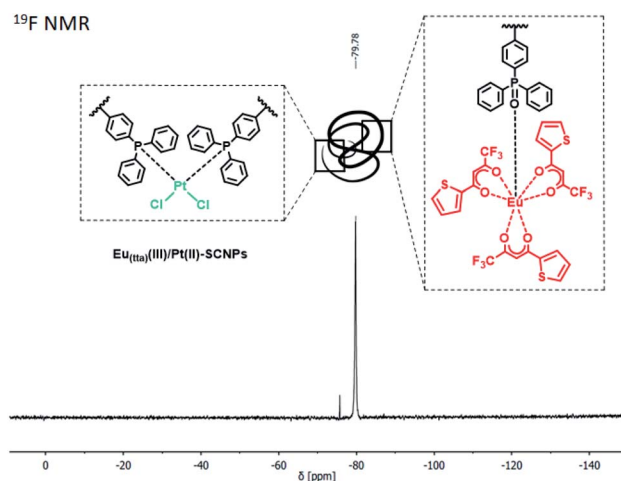
SEC analysis (THF, RI).[27] In comparison to the terpolymer **P$_{P/Oxide}$**, the SEC trace for the **Eu$_{(dbm)}$(III)/Pt(II)–SCNPs** is shifted towards longer retention times (Fig. 3, top), indicating a smaller hydrodynamic radius and thus pointing to the formation of nanoparticles without intermolecular side reactions. Further, the curve indicates the existence of a small molecular species (not shown in the spectrum), which most likely originates from unbound europium(III) complexes. To some extent the phosphine oxide coordination is apparently not sufficiently strong to withstand SEC measurement conditions. Consequently, the depicted SEC elugram rather represents a trace of Pt(II)-linked SCNPs. Furthermore, the transition of the linear terpolymer into a more compact nanoparticle was demonstrated by diffusion ordered spectroscopy (DOSY).[28,29] Based on the obtained diffusion coefficients, the hydrodynamic radii of the particles were calculated, applying the Stokes–Einstein equation (see ESI†). The mean hydrodynamic radius of **P$_{P/Oxide}$** resulted in r_H = 8.0 nm, whereas a radius of r_H = 1.9 nm was determined for the **Eu$_{(dbm)}$(III)/Pt(II)–SCNPs**. Interestingly, sole addition of [Eu(dbm)$_3$(H$_2$O)$_2$] to **P$_{P/Oxide}$**, resulting in the intermediate metallopolymer '**P$_{P/Oxide}$–Eu(dbm)$_3$**', affording a slightly larger hydrodynamic radius of r_H = 11.2 nm. Hence, the addition of an Eu species to **P$_{P/Oxide}$** does not seem to induce chain compaction. The results are in line with a 1 : 1 coordination ratio of Eu(III) to the phosphine oxide ligands of **P$_{P/Oxide}$**, confirming the orthogonal behavior of the two ligand moieties.

To determine the photophysical properties, photoluminescent emission (PL) spectra of the **Eu$_{(dbm)}$(III)/Pt(II)–**

Fig. 2 ^{19}F NMR spectrum of **Eu$_{(tta)}$(III)/Pt(II)–SCNPs** in CDCl$_3$. The tta moiety of the Eu(III) moiety allows tracking of the SCNPs in solution *via* ^{19}F NMR spectroscopy.
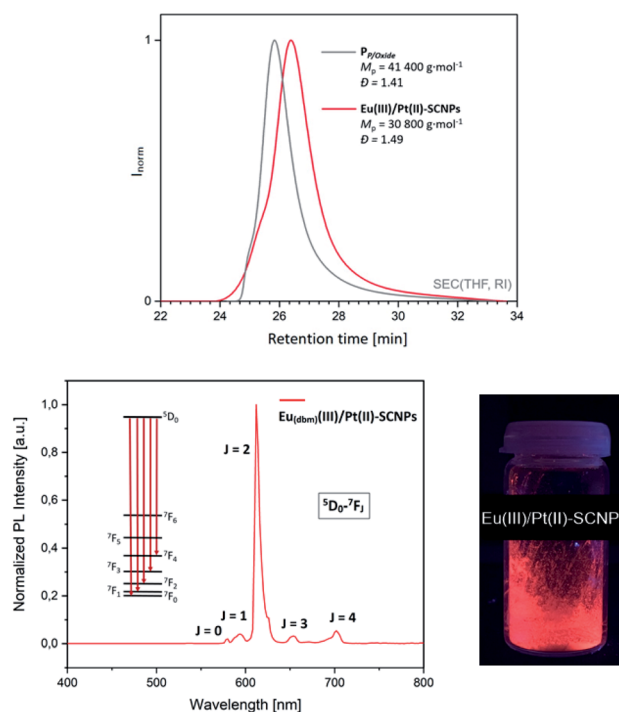
Fig. 3 SEC traces (THF, RI) of **P$_{P/Oxide}$** and the **Eu$_{(dbm)}$(III)/Pt(II)–SCNPs** (top). Photoluminescence emission (PL) spectrum of **Eu$_{(dbm)}$(III)/Pt(II)–SCNPs** (298 K) in the solid state, after excitation at λ = 350 nm (bottom).

SCNPs were recorded in the solid state (Fig. 3, bottom). After excitation at $\lambda = 350$ nm, the spectrum features characteristic bands resulting from 4f–4f transitions ($^5D_0$–^7F_J) and is dominated by a band at $\lambda = 612$ nm ($^5D_0$–$^7F_2$ transition).[25,30] The resulting bright red luminescence is typical for europium(III) compounds.[17,31] The coordination of phosphine oxide moieties to Eu(III)-diketonates is reported to further enhance the luminescence, working as an antenna ligand.[21,25] As 4f–4f transitions are virtually unaffected by the surrounding ligands of Eu(III), an almost identical emission spectrum is observed for the **Eu$_{(tta)}$(III)/Pt(II)–SCNPs** (see ESI, Fig. S26†). However, the nonsymmetric tta moiety of the Eu(III) species results in a visibly more intense luminescent behavior of the corresponding nanoparticles.

Furthermore, the **Eu$_{(dbm)}$(III)/Pt(II)–SCNPs** were characterized by multinuclear NMR spectroscopy, primarily to gain closer insights into the metal coordinated folding units. In the $^{31}P\{^1H\}$ NMR spectrum (CDCl$_3$) of the SCNPs, the resonance of the triarylphosphines at $\delta = -6.2$ ppm (Fig. 4A) is not detected anymore. Instead, an intense resonance at $\delta = 13.5$ ppm is observed, accompanied by platinum(II) satellites (d, $^1J_{P,Pt} = 3661$ Hz), which are attributed to square planar cis-[PtCl$_2$(PPh$_2$Ar)$_2$] folding units (Fig. 4B).

A minor resonance at $\delta = 19.5$ ppm is assigned to the corresponding trans-species. The obtained data are in agreement with isostructural Pt(II)–SCNPs and analogous model complexes.[8,32] The high preference for a cis-geometry of the Pt(II) centers, approx. 30 : 1 (cis/trans), is rationalized by the

Fig. 4 (A) $^{31}P\{^1H\}$NMR spectrum of **P$_{P/Oxide}$**, exhibiting resonances for the triarylphosphine and triarylphosphine oxide species in a ratio of approx. 2 : 1. (B) The $^{31}P\{^1H\}$ NMR spectrum of the **Eu$_{(dbm)}$(III)/Pt(II)–SCNPs** depicts resonances for mainly cis-coordinated [PtCl$_2$(PPh$_2$Ar)$_2$] units, with the corresponding ^{195}Pt satellites. The resonance at $\delta = 29.1$ ppm is attributed to the Eu(III) complexed phosphine oxide species.

predetermined arrangement of the precursor complex cis-[PtCl$_2$(cod)] as well as the steric constraints of the polymer backbone. Furthermore, the resonance at $\delta = 29.1$ ppm, corresponding to the phosphine oxide moieties, is still present. However, in comparison to **P$_{P/Oxide}$**, the resonance is broadened, resulting in a decrease in its integral value. This is presumably caused by the coordination to the paramagnetic europium(III) cores.[33] This effect is also observed in the alike $^{31}P\{^1H\}$ NMR spectrum of the **Eu$_{(tta)}$(III)/Pt(II)–SCNPs** (ESI, Fig. S8†). In the ^{195}Pt NMR spectrum of the **Eu$_{(dbm)}$(III)/Pt(II)–SCNPs**, a triplet resonance for the cis-[PtCl$_2$(PPh$_2$Ar)$_2$] folding units is detected at $\delta = -4420$ ppm (t, $^1J_{Pt,P} = 3715$ Hz), confirming the obtained $^{31}P\{^1H\}$ NMR data (ESI, Fig. S6†). The coordination of [Eu(dbm)$_3$] to the phosphine oxide moieties of **P$_{P/Oxide}$** is additionally evidenced by ^1H NMR spectroscopy. In the corresponding spectrum a characteristic high field resonance at $\delta = 16.9$ ppm is attributed to the methine group of the dbm ligands (ESI, Fig. S4†). Further information was obtained by IR spectroscopy. In the IR spectrum of the **Eu$_{(dbm)}$(III)/Pt(II)–SCNPs** bands for the dbm ligands are detected at $\tilde{\nu} = 1519$ cm^{-1}, 1549 cm^{-1} and 1600 cm^{-1} (ESI, Fig. S23†), pointing towards its successful encapsulation in **P$_{P/Oxide}$**.

Catalytic application

As a proof-of-principle, both synthesized heterometallic **Eu(III)/Pt(II)–SCNPs** were subsequently investigated as homogeneous catalytic systems in the amination reaction of allyl alcohol (for details refer to ESI†).[34] A similar catalytic study has previously been reported for sole Pt(II)–SCNPs, which proved to be an active and recyclable system for this reaction.[8] Yet in the current approach, the additional Eu(III) functionalities of the heterometallic SCNPs enable a photophysical detection of the catalyst via illumination with UV-light. This allows e.g. a facile verification of catalyst separation. As mentioned before, the nanoparticles featuring the tta modified Eu(III) complexes exhibited a visibly more intense luminescence, thus being more suitable as a luminescent sensor for the catalytic reaction. Aniline and allyl alcohol were employed as starting material, using 4 mol% of catalyst (equals 2 mol% of Eu species) and ferrocene as an internal standard (Fig. 5, top). These comparatively high catalyst loadings were applied mainly with regards to the amount of Eu(III) species, as the luminescence is partially quenched by the starting materials. The reaction was performed in an NMR Young tube and the respective conversion was determined by ^1H NMR spectroscopy (ESI, Fig. S28–S32†). A temperature of approx. 100 °C led to a near quantitative allyl alcohol conversion within less than 48 h, whereat merely small differences were observed for the [Eu(tta)$_3$] and [Eu(dbm)$_3$] modified SCNP systems. In each case, the mono allyl-substituted amine was predominantly generated (>80%).

The results are similar to the data obtained for the literature-known Pt(II)–SCNPs as well as the monomeric platinum complex cis-[Pt(PPh$_3$)$_2$Cl$_2$], yet a different reaction procedure and catalyst loading need to be considered when compared in detail.[8] After the catalytic reaction, the SCNPs were readily isolated by precipitation in methanol, or subsequent column
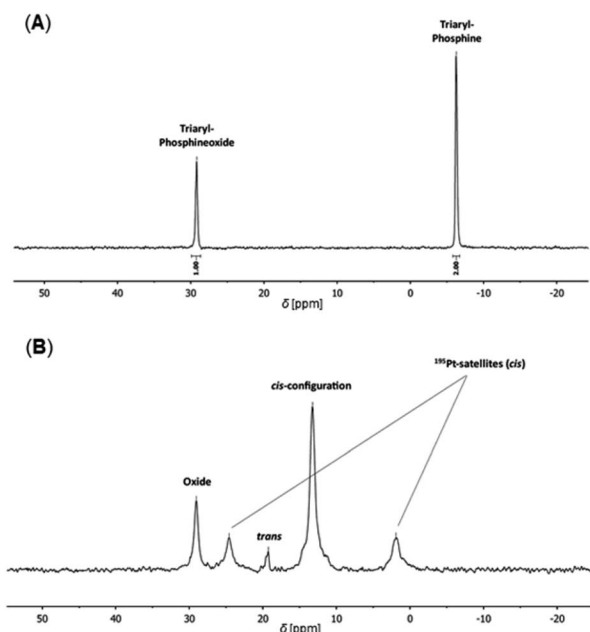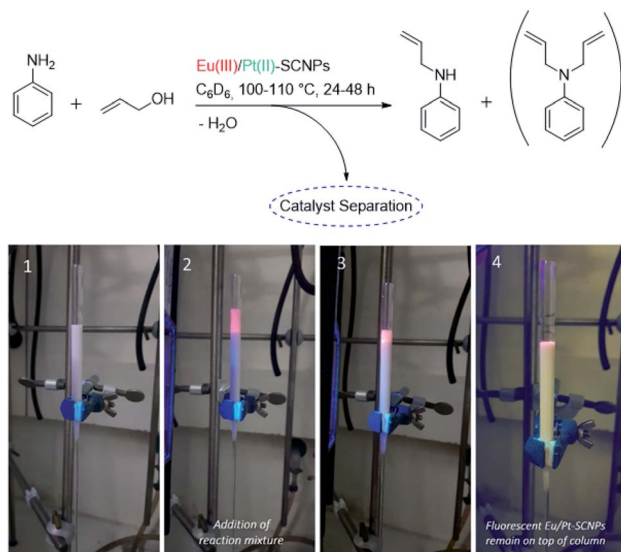
Fig. 5 (Top): Reaction of aniline with allyl alcohol catalyzed by Eu(III)/Pt(II)–SCNPs. (Bottom): Exemplary separation of the Eu(tta)(III)/Pt(II)–SCNPs via a short column chromatography (neutral aluminium oxide; acetone) subsequent to the catalytic reaction. Photographs were taken upon illumination with an UV-lamp ($\lambda_{exc.}$ = 365 nm). Picture 2 marks the addition of the reaction mixture to the column.

chromatography (e.g. acetone, neural aluminum oxide). In the latter case, they remained on top of the column and were readily detected when irradiated with UV light (Fig. 5, applying **Eu(tta)(III)/Pt(II)–SCNPs** as catalyst). Thus, for this specific reaction a simple detection mode for the catalyst's separation was achieved. UV illumination of the filtrate after column chromatography showed no luminescence, thus indicating a complete catalyst separation. However, the photoluminescence of the catalyst is visibly reduced during catalysis, most likely due to the formation of H_2O and thermal decomposition, leading to partial quenching of the Eu(III) species over time (ESI, Fig. S33†). Thus, recycling of the catalyst, as it has been previously studied for Pt(II)–SCNPs,[8] was not further pursued, as the luminescence was significantly reduced in the second cycle. Additionally, in case of the **Eu(tta)(III)/Pt(II)–SCNPs** ^{19}F NMR studies revealed that the diketonate ligands of the Eu(III) complex are partially removed with increasing reaction temperature and time. Additionally, in the eluant of the chromatography a weak resonance in the ^{19}F NMR spectrum is detected, attributed to unbound tta ligands, confirming partial decomposition during catalysis.

Advantageously, the amount of phosphine and phosphine oxide moieties can readily be adjusted. Thus, for future studies, an introduction of task-specific quantities of Pt(II) and Eu(III) centers, as well as the implementation of other metal combinations, is feasible.

Conclusions

In summary, a bifunctional terpolymer containing two orthogonal ligand moieties was synthesized via NMP, giving way to the facile formation of heterometallic **Eu(III)/Pt(II)–SCNPs**. The SCNP synthesis proved to be selective in metal coordination and independent from the sequence of metal addition. In addition, featuring catalytic and luminescent centers, the SCNPs were employed as a homogeneous catalytic system. The selective coordination of two metal species exhibiting different functionalities represents, to this date, an unprecedented concept in the realm of single-chain nanoparticles. The combinatorial design of catalytically active and luminescent properties within a SCNP system may not only allow the visualization of the catalyst (and its separation), yet tracking for specific systems seems practicable.

Conflicts of interest

There are no conflicts to declare.

Acknowledgements

Notes and references

1 S. Mavila, O. Eivgi, I. Berkovich and N. G. Lemcoff, *Chem. Rev.*, 2016, **116**, 878.

2 A. M. Hanlon, C. K. Lyon and E. B. Berda, *Macromolecules*, 2016, **49**, 2.

3 C. K. Lyon, A. Prasher, A. M. Hanlon, B. T. Tuten, C. A. Tooley, P. G. Frank and E. B. Berda, *Polym. Chem.*, 2015, **6**, 181.

4 I. Berkovich, S. Mavila, O. Iliashevsky, S. Kozuch and N. G. Lemcoff, *Chem. Sci.*, 2016, **7**, 1773.

5 Y. Liu, P. Turunen, B. F. M. de Waal, K. G. Blank, A. E. Rowan, A. R. A. Palmans and E. W. Meijer, *Mol. Syst. Des. Eng.*, 2018, **3**, 609.

6 J. Rubio-Cervilla, E. González and J. Pomposo, *Nanomaterials*, 2017, **7**, 341.

7 H. Rothfuss, N. D. Knöfel, P. W. Roesky and C. Barner-Kowollik, *J. Am. Chem. Soc.*, 2018, **140**, 5875.

8 N. D. Knöfel, H. Rothfuss, J. Willenbacher, C. Barner-Kowollik and P. W. Roesky, *Angew. Chem., Int. Ed.*, 2017, **56**, 4950.

9 A. Sanchez-Sanchez, A. Arbe, J. Colmenero and J. A. Pomposo, *ACS Macro Lett.*, 2014, **3**, 439.

10 T. Terashima, T. Mes, T. F. A. De Greef, M. A. J. Gillissen, P. Besenius, A. R. A. Palmans and E. W. Meijer, *J. Am. Chem. Soc.*, 2011, **133**, 4742.

11 S. Mavila, I. Rozenberg and N. G. Lemcoff, *Chem. Sci.*, 2014, **5**, 4196.

12 S. Thanneeru, J. K. Nganga, A. S. Amin, B. Liu, L. Jin, A. M. Angeles-Boza and J. He, *ChemCatChem*, 2017, **9**, 1157.

13 J. Chen, K. Li, J. S. L. Shon and S. C. Zimmerman, *J. Am. Chem. Soc.*, 2020, **142**, 4565.

14 J. Chen, J. Wang, K. Li, Y. Wang, M. Gruebele, A. L. Ferguson and S. C. Zimmerman, *J. Am. Chem. Soc.*, 2019, **141**, 9693.

15 Y. Liu, S. Pujals, P. J. M. Stals, T. Paulöhrl, S. I. Presolski, E. W. Meijer, L. Albertazzi and A. R. A. Palmans, *J. Am. Chem. Soc.*, 2018, **140**, 3423.

16 J. P. Cole, A. M. Hanlon, K. J. Rodriguez and E. B. Berda, *J. Polym. Sci., Part A: Polym. Chem.*, 2017, **55**, 191.

17 H. Rothfuss, N. D. Knöfel, P. Tzvetkova, N. C. Michenfelder, S. Baraban, A.-N. Unterreiner, P. W. Roesky and C. Barner-Kowollik, *Chem.–Eur. J.*, 2018, **24**, 17475.

18 N. D. Knöfel, H. Rothfuss, C. Barner-Kowollik and P. W. Roesky, *Polym. Chem.*, 2019, **10**, 86.

19 Y. Liu, T. Pauloehrl, S. I. Presolski, L. Albertazzi, A. R. A. Palmans and E. W. Meijer, *J. Am. Chem. Soc.*, 2015, **137**, 13096.

20 J. Willenbacher, O. Altintas, V. Trouillet, N. Knöfel, M. J. Monteiro, P. W. Roesky and C. Barner-Kowollik, *Polym. Chem.*, 2015, **6**, 4358.

21 A. W. G. Platt, *Coord. Chem. Rev.*, 2017, **340**, 62.

22 C. J. Hawker, G. G. Barclay and J. Dao, *J. Am. Chem. Soc.*, 1996, **118**, 11467.

23 L. Daasch and D. Smith, *Anal. Chem.*, 1951, **23**, 853.

24 M. Halmann and S. Pinchas, *J. Chem. Soc.*, 1958, 3264.

25 N. B. D. Lima, S. M. C. Gonçalves, S. A. Júnior and A. M. Simas, *Sci. Rep.*, 2013, **3**, 2395.

26 H. Yasuchika, T. Shiori, Y. Masanori, N. Takayuki, K. Yuichi, S. Tomohiro, I. Hajime and F. Koji, *Chem. - Eur. J.*, 2017, **23**, 2666.

27 J. Engelke, J. Brandt, C. Barner-Kowollik and A. Lederer, *Polym. Chem.*, 2019, **10**, 3410.

28 E. Blasco, B. T. Tuten, H. Frisch, A. Lederer and C. Barner-Kowollik, *Polym. Chem.*, 2017, **8**, 5845.

29 P. Groves, *Polym. Chem.*, 2017, **8**, 6700.

30 E. Moretti, L. Bellotto, M. Basile, C. Malba, F. Enrichi, A. Benedetti and S. Polizzi, *Mater. Chem. Phys.*, 2013, **142**, 445.

31 K. Binnemans, *Coord. Chem. Rev.*, 2015, **295**, 1.

32 L. Bemi, H. C. Clark, J. A. Davies, C. A. Fyfe and R. E. Wasylishen, *J. Am. Chem. Soc.*, 1982, **104**, 438.

33 N. B. D. Lima, A. I. S. Silva, P. C. Gerson Jr, S. M. C. Gonçalves and A. M. Simas, *PLoS One*, 2016, **10**, e0143998.

34 S. Bähn, S. Imm, L. Neubert, M. Zhang, H. Neumann and M. Beller, *ChemCatChem*, 2011, **3**, 1853.